Journal of Sound and Vibration (2002) **249**(2), 351–370
doi:10.1006/jsvi.2001.3845, available online at http://www.idealibrary.com on IDEAL®

AEROACOUSTIC RESEARCH IN EUROPE: THE CEAS-ASC REPORT ON 2000 HIGHLIGHTS

S. IANNIELLO

INSEAN – Italian Ship Model Basin Via di Vallerano, 139, 00128 *Rome*, *Italy*.
E-mail: *s.ianniello@insean.it*

(*Received* 13 *June* 2001, *and in final form* 13 *June* 2001)

This paper summarizes the highlights of aeroacoustics research in Europe in 2000, compiled from information provided to the CEAS Aeroacoustics Specialists' Committee (ASC). The Confederation of European Aerospace Societies (CEAS) comprises the national Aerospace Societies of France (AAAF), Germany (DGLR), Italy (AIDAA), the Netherlands (NVvL), Spain (AIAE), Sweden (FTF), Switerland (SVFW), and the United Kingdom (RAeS).

1. INTRODUCTION

The role of the CEAS Aeroacoustics Specialists' Committee (ASC) is to serve and support the scientific and industrial aeroacoustics community in Europe. Here "Aeroacoustics" is to encompass all aerospace acoustics and related areas. Each year the Committee will highlight some of the research and development activities in Europe. This is the report of the 2000 highlights; contributions to this report have been made by the following people: S. Oerlemans, P. Sijtsma, J. Delfs, T. Lauke, W. Dobrzynski, W. Neise (*DLR*), Peter Költzsch (*Technical University Dresden*), H. Batard (*EADS*), C. Bogey, C. Bailly, D. Juvé (*Ecole Centrale de Lyon*), W. Just, I. U. Borchers (*Dornier GmbH*), D. Gély, G. Elias, C. Bresson, S. Lewy, J. Prieur, G. Rahier, P. Spiegel, P. Malbéqui (*ONERA*), H. Foulon (*CEAT*), G. Guidati, S. Wagner (*IAG*, *University of Stuttgart*), F. Kennepohl (*Münich Technical University*), A. Roure, A. Albarrazin, M. Winninger (*LMA*), A. de Boer, H. Tijdeman, F. van der Eerden, T. Basten (*University of Twente*).

2. AIRFRAME NOISE

2.1. EFFECTS OF WIND TUNNEL SIDE-PLATES ON AIRFRAME NOISE

The effects of wind tunnel side-plates on airframe noise measurements with phased arrays were investigated both experimentally (in NLR's Small Anechoic Wind Tunnel) and theoretically [1]. In a previous set-up, with acoustically hard side-plates and a cross-shaped array, calibration measurements with a monopole source showed differences between array output and actual source strength up to 10 dB, with strong dependence on frequency and source location. Theory predicted much better results when the cross-shaped array was replaced by a sparse array and the hard plates by acoustically lined plates. After application of these modifications in the test set-up, new calibration measurements indeed showed impressive improvement in the ability to determine absolute levels with a phased array

0022-460X/02/020351 + 20 $35.00/0

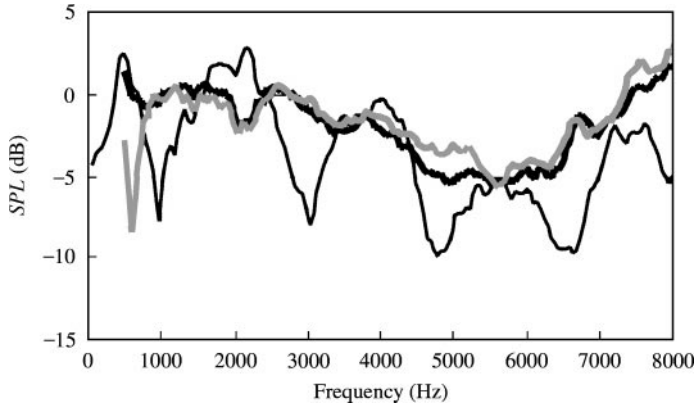

Figure 1. Monopole source levels determined with phased microphone array, in an anechoic environment (i.e., actual source strength), in the previous set-up (hard side-plates/cross array), and in the new set-up (lined side-plates/sparse array): ▬, anechoic; ▬, previous set-up; ▬, new set-up.

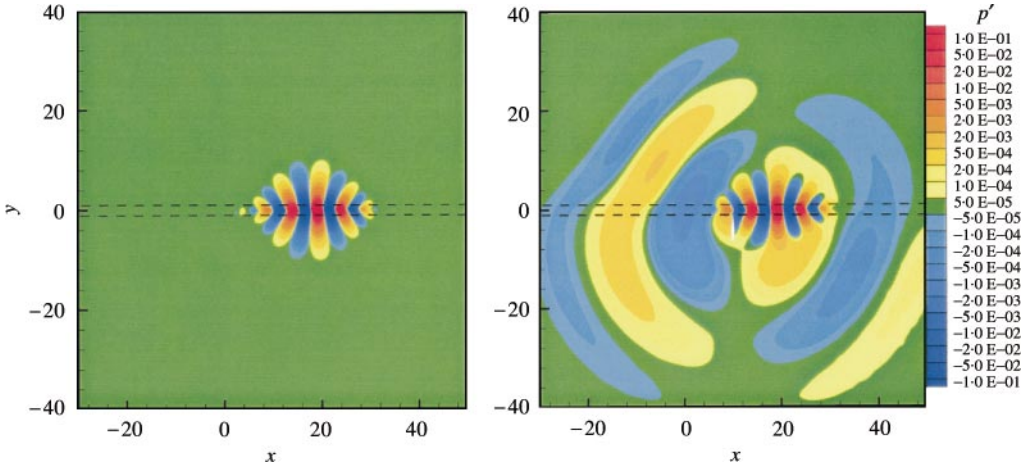

Figure 2. Pressure of wave packet evolving along shearlayer. Left: free, right: with edge.

(within 2 dB), independent of frequency or source position (see Figure 1) (by S. Oerlemans and P. Sijtsma).

2.2. CAA SIMULATION OF SOUND GENERATION BY LINEAR INTERACTION OF VORTICITY WITH A WEDGE

The study of airframe noise is intimately connected with the interaction of flow with edges. In this context the question arises whether linearized conservation equations describe such sources. Lilley's aeroacoustic wave equation states that in a subsonic parallel steady mean shear flow $\mathbf{u}^0 = [u_1, u_2, u_3]^0 = [u_1^0(x_2), 0, 0]$ sound is generated by non-linear processes only, because the respective aeroacoustic source term $\partial u_i/\partial x_l\, \partial u_k/\partial x_i\, \partial u_l/\partial x_k$ vanishes upon linearization about the basic state $\mathbf{u}^0$. The linear dynamics of any small perturbations $\mathbf{u}'$, e.g., due to small fluctuations of the vorticity, will therefore not contribute

to the generation of noise. In order to verify the above statement a numerical simulation of the linear dynamics of a purely vortical perturbation evolving in a free parallel shearlayer was carried out using DLR's CAA Chimera code [2] (see also reference [3]). The shearlayer is located in $-1{\cdot}1 \leqslant x_2 \leqslant 1{\cdot}1$; below there is no flow and above there is a uniform flow of Mach number $M = 0{\cdot}4$. Localized vorticity is introduced at simulation time $t = 0$ and position $x = x_1 = 2$, $y = x_2 = -0{\cdot}5$. As a result, a downstream convecting unstable wave packet evolves representing the classical Kelvin–Helmholtz instability. The left-hand side of Figure 2 shows the respective linear pressure field $p'(x, y, t = 70)$, which consists of purely hydrodynamic (i.e., non-propagating) components indicating complete silence and thus confirming the statement Lilley's equation. The righthand side of Figure 2 shows the pressure field if a sharp vertical wedge with vertex at $x = 10$, $y = -1{\cdot}4$ is originally placed below the shear layer. In this case sound is generated by scattering of the wave packet's linear hydrodynamic pressure field at the wedge although the mean flow does not even touch the wedge. The example shows that in the presence of edges the sound generation by vorticity becomes a linear problem even in the presence of a parallel shear flow (by J. Delfs and T. Lauke).

2.3. AIRFRAME NOISE FROM WING HIGH-LIFT DEVICES: SUCCESSFUL PREDICTION OF FULL-SCALE FLYOVER NOISE FROM (DNW) MODEL-SCALE STUDIES

A good knowledge of aircraft noise characteristics (spectra and directivities) is indispensable in predicting noise emission contours around airports. Since during landing approach the total aircraft noise is not solely determined by the engines, but much rather by flow around the entire airframe, the specific characteristics of both engine- and airframe-related noise components need to be determined.

Engine noise signatures are well documented by the manufacturers. In contrast, airframe noise characteristics (specifically related to landing gears and wing high-lift devices) were yet unknown in necessary detail. Within a dedicated German national program high-lift device (HLD) airframe noise signatures were determined from scale-model experiments on complete aircraft configurations in the German–Dutch Wind Tunnel (DNW) both in terms of spectra and of directivities in longitudinal and azimuthal directions. After transformation to full scale the wind tunnel results compare well with flyover noise data for an aircraft with

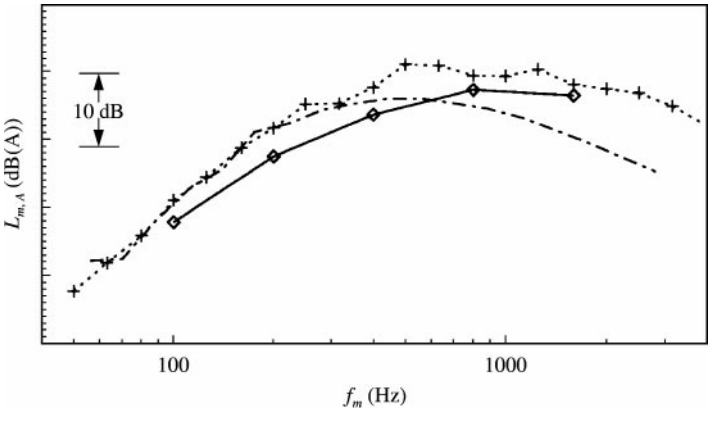

Figure 3. Comparison of wing high-lift device airframe noise spectra from fly-over and scale-model wind tunnel tests. ◇——◇, Fink prediction; +·····+ , flyover noise data; –·–·–, prediction from wind tunnel experiment.

its HLD fully deployed. An example is provided in Figure 3 showing wing HLD noise spectra in the vertical radiation direction (i.e., for the aircraft directly overhead). While at low frequencies flyover and wind tunnel data exhibit excellent agreement, an increasing offset is observed at higher frequencies. This could well be expected since accompanying wind tunnel tests on full-scale aircraft wings showed conclusively that excess noise occurs from small structural components, whose detailed geometry simply cannot be reproduced at model scale. It is worth mentioning that good agreement between flyover and wind tunnel data is also obtained with respect to the noise directivity, exhibiting maximum levels in the rear arc as a result of noise radiation from the deployed wing slats (by W. Dobrzynski).

2.4. FIRST PHASE OF GERMAN RESEARCH INITIATIVE INTO THE COMPUTATION OF AIRFRAME NOISE SUCCESSFULLY COMPLETED

The aim of the co-operative national research initiative SWING (Simulation of Wing-flow Noise Generation) is the computation of airframe noise generated at the high-lift devices of modern transport aircraft at approach conditions. Within the first 3 years of the project the partners from three German universities (Aerodynamisches Institut RWTH, Aachen, Institut für Aerodynamik und Gasdynamik University, Stuttgart, Institut für Akustik und Sprachkommunikation University of Technology, Dresden) and DLR (Institut für Entwurf-saerodynamik) have developed and validated computational approaches based on (1) the numerical solution of an acoustic wave equation (BEM) in combination with statistical source modelling and (2) the high-accuracy numerical solution (CAA) of 3-D linearized Euler equations (LEE) for a direct simulation of perturbations about the mean flow field and thus the sound generation process.

In this first project phase the methods were successfully tested against CAA benchmark problems and problems of edge noise generation (leading edges and trailing edges). Respective aeroacoustic validation tests were carried out in the aerodynamic wind tunnels of University, Stuttgart as well as the anechoic tunnels of TU, Dresden and DLR Braunschweig employing microphone arrays and acoustic mirrors for source localization. Moreover, source data were also generated by means of Large Eddy Simulation of the turbulent fluctuations near a trailing edge in order to validate the statistical source model of the acoustic analogy approach as well as the stochastic fluctuation model used in the LEE. The project was funded partially by the Deutsche Forschungsgemeinschaft DFG, the ministry of research and education (BMBF) as well as DLR. Research progress was documented within two international colloquia held in Dresden 1999 and Braunschweig 2000, the proceedings [4, 5] of which are available through either of the two authors (by P. Költzsch and J. Delfs).

3. FAN AND JET NOISE

3.1. RESEARCH ON THE NACELLE DEVICES TO REDUCE THE FAN NOISE

The RANNTAC project started in January 1998 and finished as planned in December 2000. The objective of this project was to acquire the technology necessary to support the design and the manufacturing of turbofan engine nacelles featuring innovative noise reduction devices. During these 3 years, the following families of concepts have been studied: (1) passive liners including an investigation of non-locally reacting concepts; (2) adaptive liners; (3) negatively scarfed intake; (4) active noise control including actuator technology.

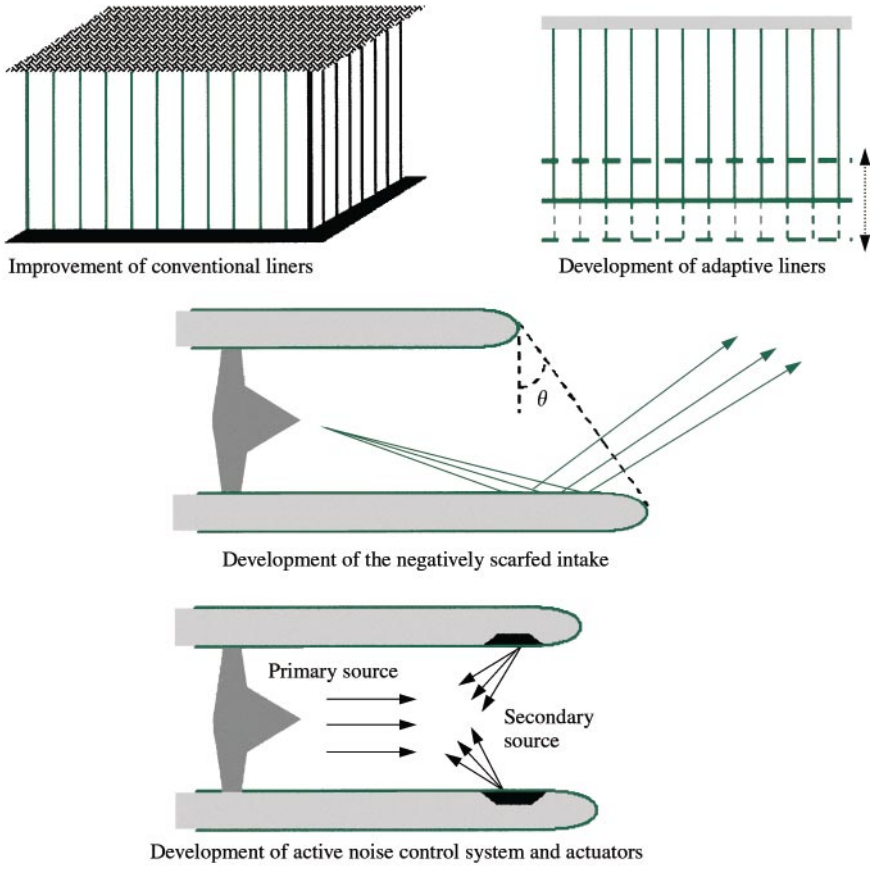

Figure 4. Sketches of concepts developed in RANNTAC project.

In view of the large number of concepts (see Figure 4), considerable efforts have been devoted to the definition of technical objectives and the formulation of an assessment procedure to guide the development of viable concepts for industrial application. A major part of the effort has been applied to the development of innovative nacelle treatment concepts, including advanced liners and the negatively scarfed intake. Extensive computations and tests have been carried out with various facilities on liner concept configurations, including full-scale tests on a real engine. Investigations have also been conducted on the manufacturing processes and to the improvement of structural properties, namely weight and bonding quality. The linear concepts have been demonstrated to widen the frequency bandwidth through careful control of the imaginary part of impedance. The effect of the real part on the attenuation has also been confirmed and the need to improve manufacturing processes to obtain a closer match to the optimum resistance has been identified.

An experimental evaluation of the negatively scarfed inlet has quantified the acoustic power and directivity changes due to the negative scarf angle, relative to that of an axisymmetric intake. The fan rig tests have shown that a significant reduction of acoustic power radiated towards the ground in the flyover plane is achieved for both tone and broadband noise, as well as important changes in the directivity pattern. It has also been shown that there is an overall reduction of acoustic power in the whole flyover plane (the

increase of noise toward sky is not as large as the decrease toward ground). This result implies a re-distribution of the noise sideways due to the scarf angle that requires further study. The development of active noise control (ANC) technology for engine nacelles, included significant work on the improvement of control algorithms and theoretical studies on the positioning and numbers of actuators/sensors with respect to modal content in the duct. The results were confirmed by testing on a fan rig, which evaluated the accuracy of various algorithms, their robustness with respect to engine speed variations and validated a new radial mode analysis. Significant noise reductions have been measured for low-frequency tones (1 BPF) but tests and theoretical studies show that harmonics will be more difficult to reduce because of the much higher number of propagating modes. Actuators suitable for Nacelle Active Noise Control have also been thoroughly studied. Significant improvements have been achieved in the weight, volume and power consumption required to achieve reasonable acoustic levels.

Aircraft noise impact studies have been carried out to enable conclusions to be drawn concerning further improvements or future studies for each of the concepts. These will be of considerable use to forthcoming industrial or research programs on aircraft noise reduction (by H. Batard).

3.2. DIRECT SIMULATION OF AERODYNAMIC NOISE

The noise radiated by turbulent flows was investigated through direct simulation [6–8] with the two illustrations of a 2-D cavity and a 3-D jet. In order to obtain the acoustic field directly, a code solving the compressible Navier–Stokes equations was developed using specific numerical techniques, such as the DRP scheme of Tam and Webb for space integration and a fourth order Runge–Kutta algorithm for time advancement. The boundary conditions of Tam and Dong are implemented in combination with a sponge region at the outflow boundary. First, a 2-D open cavity with a laminar incoming boundary layer with a Mach number of 0·5 was simulated by DNS [8]. Figure 5 presents the acoustic field generated by instability waves of the shear layer impinging the downstream corner

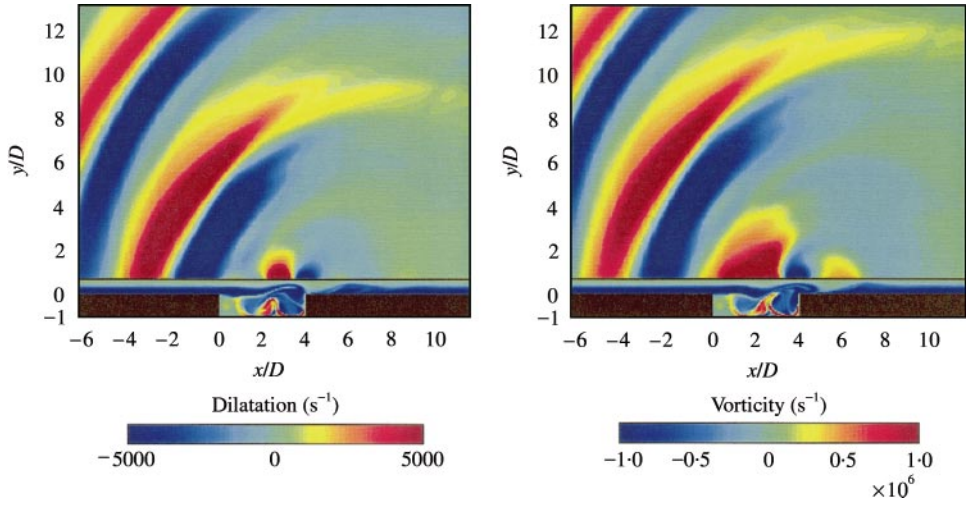

Figure 5. Visualization of the dilatation field in the upper part and of the vorticity field in the lower part for two successive times with a ratio $L/\delta_{\theta 1} \simeq 63$.

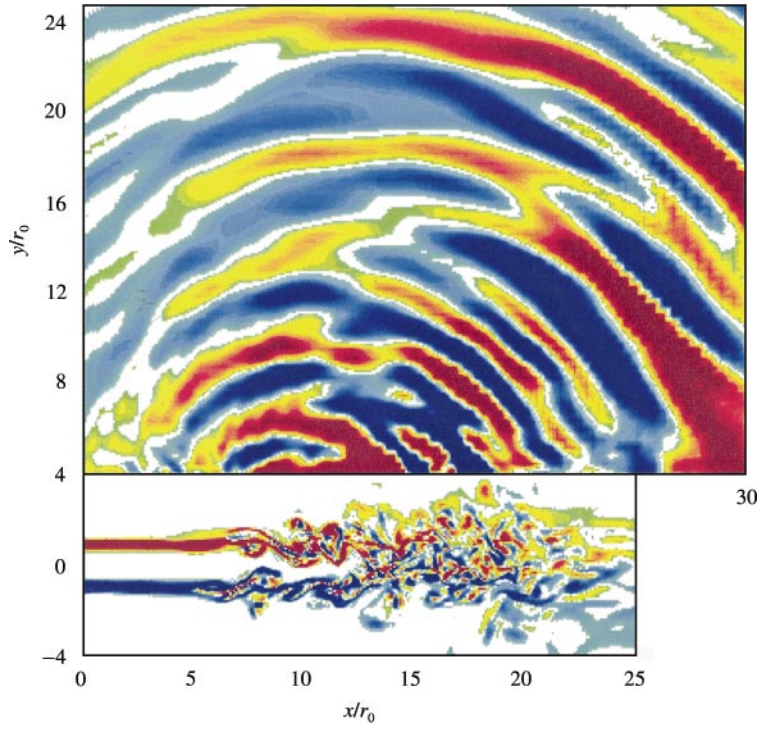

Figure 6. Snapshot of the dilatation field $\Theta = \nabla \cdot v$ in the acoustic region, and of the vorticity field ω_{xy} in the aerodynamic region, in the $x - y$ plane at $z = 0$. The dilatation color scale is defined for levels from -90 to $90\ s^{-1}$.

(X. Gloerfelt, *Ph.D. Thesis*). Second, a Mach 0·9, Reynolds number 6×10^4, 3-D round jet is simulated by LES [6] (see Figure 6). The aerodynamic properties of the jet, such as meanflow parameters and turbulent intensities, are in very good agreement with experimental data. The sound field generated by the jet is obtained directly in the simulation and investigated. Acoustic sources in the jet are located around the end of the potential core, consistent with experimental observations. Radiation directivity and sound levels are compared successfully with corresponding measurements (by C. Bogey, C. Bailly and D. Juvé).

3.3. SUCCESSFUL TESTING OF ACTIVE STATORS FOR TURBOFAN ENGINES IN EUROPE

Within the EC funded project RESOUND (Reduction of engine source noise through understanding and novel design) very promising results could be achieved in testing of Active Stators for reduction of tonal rotor/stator interaction noise in the fan of aeroengines. The Active Stators were developed by Dornier GmbH/Germany and successfully tested in a model-scale fan rig of SNECMA/France in co-operation with EADS Deutschland Corporate Research Center (see Figure 7). The actuators are flush mounted on and integrated in the stator vanes of a model-scale fan rig to act as control devices nearest to the source of the rotor–stator interaction noise caused by the viscous wakes of the rotor (see small picture in Figure 7) . Results of a first test campaign show averaged reductions of up to 15 dB at BPF in a selected area of interest in the upstream farfield at lower frequencies (1500 Hz, see Figure 8). In the remaining upstream farfield the control is nearly global. Furthermore, the SPL maps gathered with an upstream moving far field antenna show that

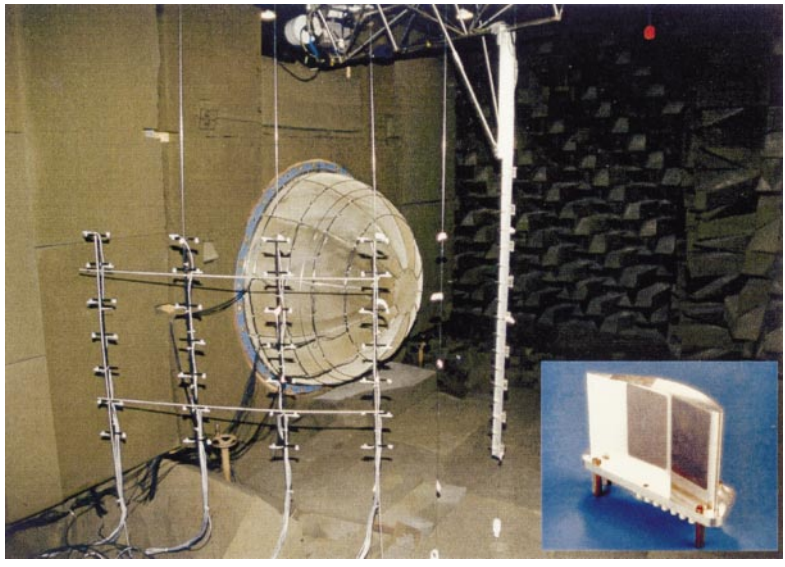

Figure 7. Monitor microphones and Active Stator vane for Active Stator testing.

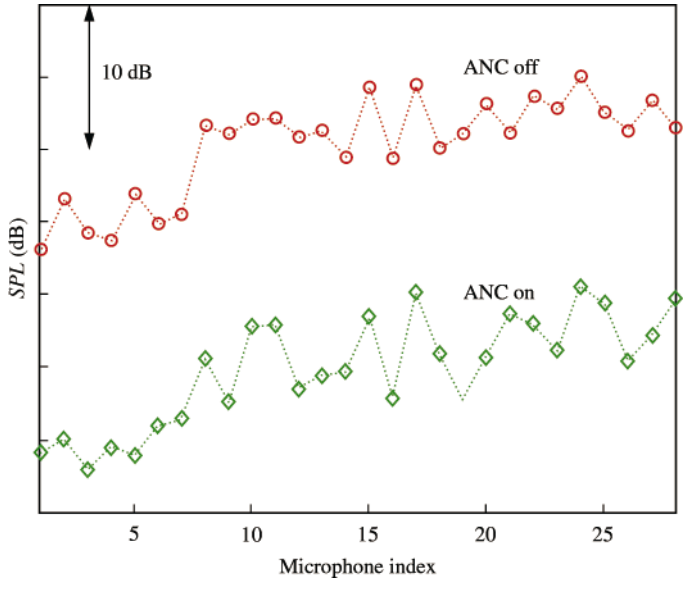

Figure 8. Active Stator testing. Selected sound pressure levels measured at Dornier static farfield microphones.

a good reduction at high angles to the machine axis is achieved in nearly each test case (by W. Just and I. U. Borchers).

3.4. SOUND PRESSURE LEVEL REDUCTION AROUND THE ARIANE 5 LAUNCH VEHICLE

The vibroacoustic tests made during the last V503 qualification flight of the Ariane launcher (October 1998) confirmed the need to reduce, especially in the 31·5 Hz octave

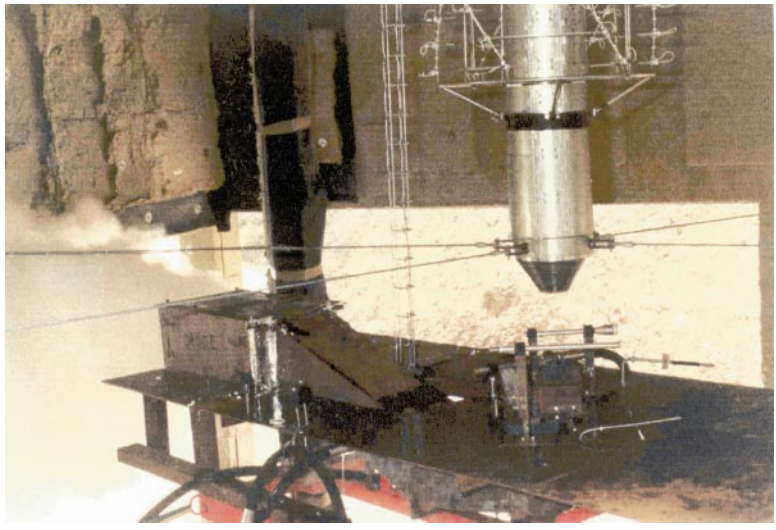

Figure 9. Ariane 5 launch pad mock-up with duct extension in MARTEL facility.

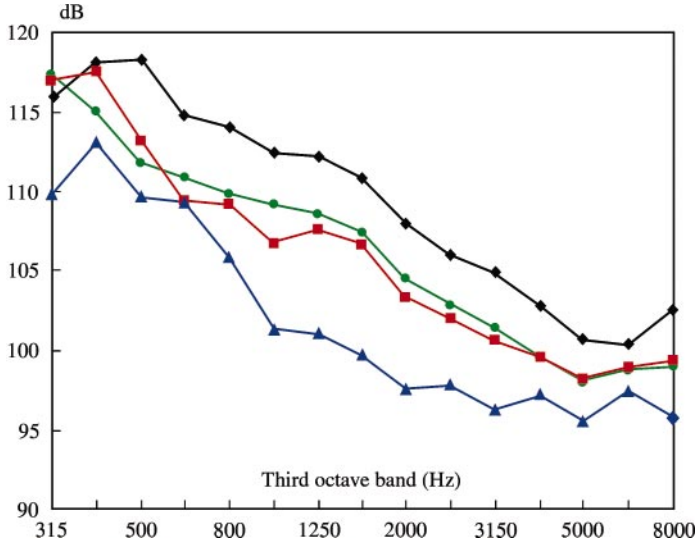

Figure 10. Duct extensions effect. —◆—, no flue extension (V503); —●—, 10-m flue extension; —■—, 15-m flue extension; —▲—, 30-m flue extension.

band, the acoustic levels underneath the fairing when the launcher goes through the altitude 10–20 m. Based on the relative levels of the Solid Rocket Booster (SRB), the central engine sources and the NR indexes, it appeared necessary to reduce the acoustic sources at the outlet of the two solid booster ducts by at least 6 dB to achieve the required noise reduction inside the fairing.

A test campaign was conducted in the MARTEL facility in 1999 to test systems which could satisfy this requirement. Two methods were investigated. The first consisted of attempting to improve the efficiency of the water injection systems even more by focusing on the incriminated source regions. Unfortunately, despite a few improvements observed in

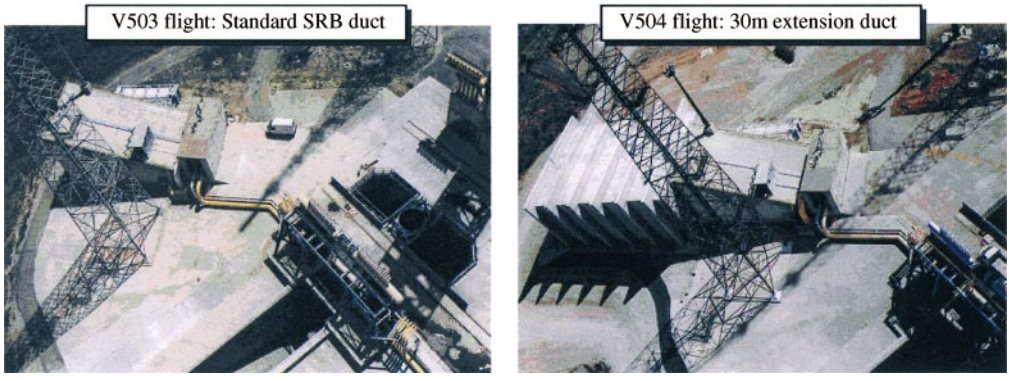

Figure 11. SRB duct extension in Kourou site.

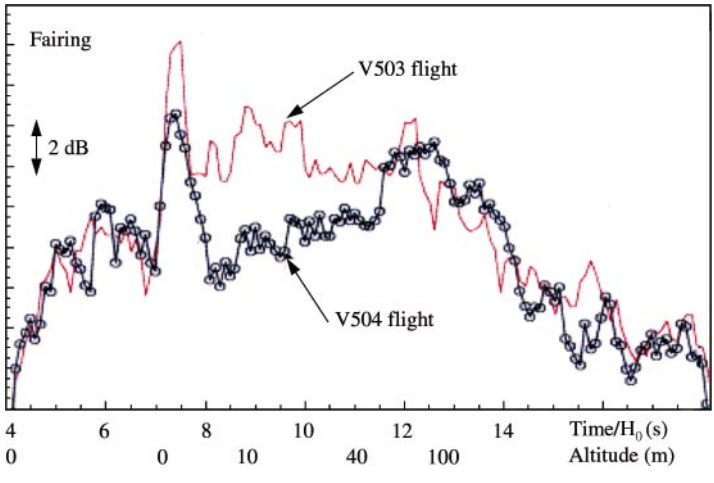

Figure 12. V503-V504 Ariane 5 flights. Acoustic data comparison.

certain configurations, the noise reductions in the frequency band concerned did not exceed 2 dB and were therefore too low to implement this type of solution. The second method investigated was an extension of the SRB ducts (see Figure 9). The noise spectra measured for three extensions 10, 15 and 30 m are shown in Figure 10. These results were obtained for a critical altitude of 10 m. In each case, a noise reduction was observed over a wide frequency band. The noise reduction increases with the duct extension length. However, based on results not presented here, the reduction decreases as the launcher climbs. Indeed, the extension of the duct gradually masks the jet near the final section. The noise attenuations observed are due to the masking effect of the duct and to the change in the direction of the jet subsequent to the horizontal extension of the duct. The main jet emission direction is thus farther from the top part of the launcher. Quantification and extrapolation of the attenuation predictable at full scale in the 31·5 Hz octave are based on the geometric scale (1 : 47), the Strouhal reduced number, which takes the velocity and temperature effects into account (1 : 42), and the velocity ratio at the duct outlet based on flow rate conservation (1 : 29). It appeared that a 30-m horizontal extension of the solid booster stage ducts satisfies the stated requirement. The building on the Kourou site was performed just before the V504 flight (see Figure 11).

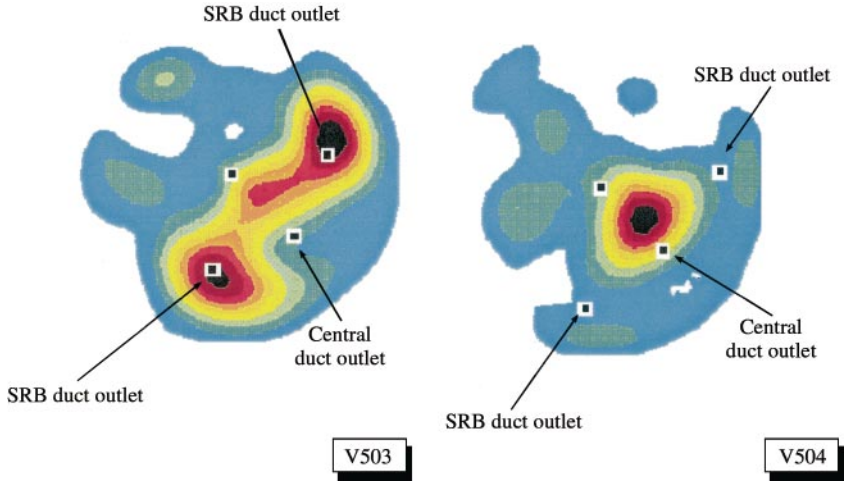

Figure 13. Acoustic sources localization V503-V504 flights. Top view.

The comparison between V503 and V504 flights appears in Figure 12. The mean sound pressure level of microphones located on the fairing has been plotted between $H_0 + 4$ s and $H_0 + 18$ s. Between $H_0 + 4$ s and $H_0 + 7$ s, when the central engine (Vulcain) in running alone, before the SRB ignition, no difference is observed. In contrast, a reduction of about 5 dB appears from $H_0 + 7$ s to $H_0 + 12$ s (60 m in altitude). It is interesting to quote that with the new extended ducts, the contribution of the SRB to the noise during this time seems to have disappeared, the levels being the same before and after their ignition. This result is confirmed by noise source localization A full microphone array consisting of 12 flush-mounted microphones has been implemented around the fairing, in order to perform noise source localization during lift-off. An example of the results is presented in Figure 13. The V504 acoustic map, compared to the V503 one, shows that no acoustic source remains at the SRB duct outlets at an altitude of 20 m. The full-scale measurements fully agree with the predictions made using the MARTEL facility, and the final noise reduction objective is reached. The MARTEL facility and expertise in advanced signal processing techniques prove to be excellent, invaluable, performing tools for successfully conducting experimental studies designed to reduce the noise level of a launcher at lift-off (by D. Gély, G. Elias, C. Bresson and H. Foulon).

3.5. ACTIVE CONTROL OF NOISE FROM TURBOMACHINES

Active noise control of turbomachinery tones up to $ka = 10$ was successfully demonstrated with a fan model of 1 m diameter, using 32 actuators and 32 error sensors wall-mounted in the inlet duct section. In this project—supported by the German Ministry for Research and Technology (BMBF) in the framework of the AG Turbo—DLR provided the test stand and executed the radial mode analysis of the sound field, EADS provided and operated a 32-channel controller using filtered-x-LMS-algorithms, and MTU Aero Engines developed a computer code to simulate the ANC sound field in the duct and specified the optimum locations of actuators and sensors (see Figure 14). Total sound power reductions of 27 dB at 340 Hz, where eight duct modes are propagational in both directions in the duct, have been achieved and 11 dB at 680 Hz, where 28 modes are propagational, using the control concept of minimizing the squared sound pressures measured at the error sensor

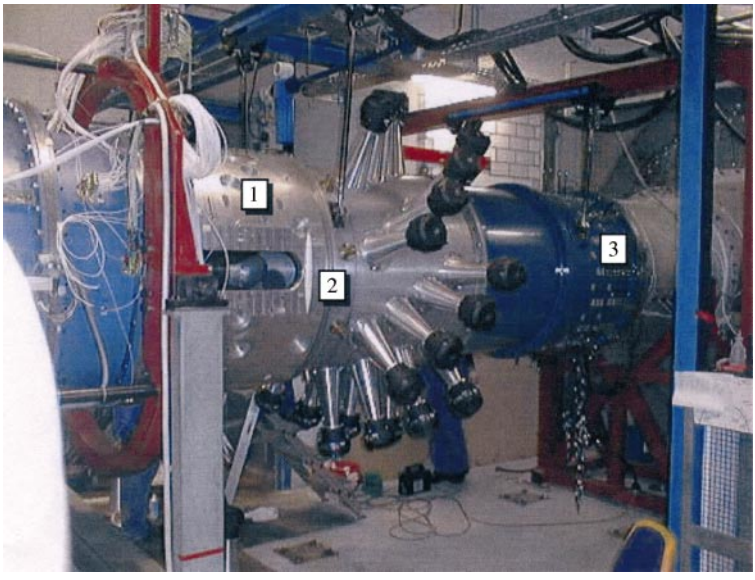

Figure 14. Fan rig at DLR with active noise control equipment: 1, Fan casing; 2, actuators; 3, sensors.

positions. Additionally, a modal control concept was successfully applied, which allows cancellation of selected azimuthal mode orders (by F. Kennepohl and W. Neise).

3.6. SUCCESSFUL TESTING OF LOW-NOISE AIRFOILS ON MODEL WIND TURBINE IN DNW

The EU-funded project DATA (Design and Testing of Acoustically Optimized Airfoils for Wind Turbines, JOR3-CT98-0248) aimed at the reduction of braodband aerodynamic noise from wind turbines. The work focused on the major noise mechanism, namely turbulent-boundary-layer-trailing-edge-interaction noise A prediction model developed by TNO-TPD allowed the design of airfoils which minimize this type of noise. In a series of wind tunnel tests on cylindrical airfoil sections it could be shown that reductions in the order of 2–4 dB are possible. This was confirmed during a test in the Large Low-speed Facility of DNW. The results indicate that noise reductions in the same order of magnitude can be expected for both tripped and untripped flow conditions, without negative effect on the power production. The approach of designing low-noise airfoils may also be applied in related areas such as fan noise (Partners: IAG, LM Glasfiber Holland, NLR, TNO-TPD, ECN) (by G. Guidati and S. Wagner).

3.7. STUDIES ON ACOUSTICS OF TURBOFANS

Main achievements at ONERA on turbofan noise have been related to broadband noise. Work has been performed in the framework of the European project RESOUND. Further analyses of the FANPAC tests made by Rolls-Royce in their anechoic facility enabled us to get more information on broadband noise [9]. Figure 15 (on the left) shows the total (including the tones) and broadband overall sound power levels, OAPWL, radiated upstream of the fan (the reference of the dB-scale is arbitrary). The difference between both curves is about 2 dB at subsonic rotation tip Mach numbers, M_{tip}, which proves that

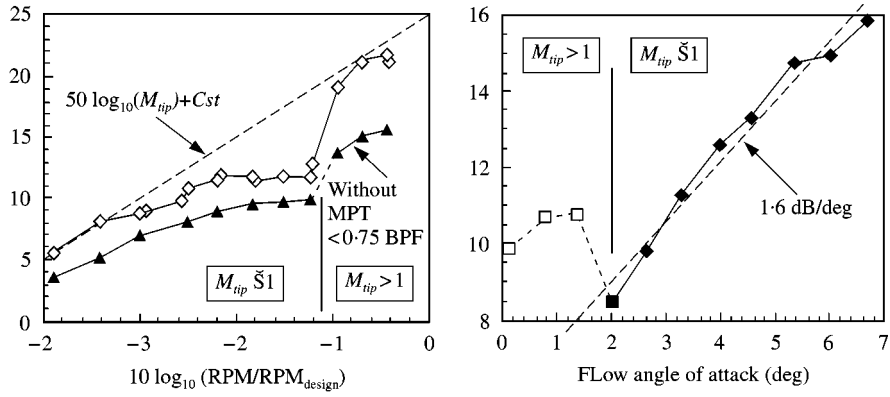

Figure 15. Left figure shows the relative overall sound power level versus rotation speed, N r.p.m. (logarithmic scale); right figure shows the reduced broadband sound power level versus the flow angle of attack on rotor blades. —◇—, Total; —▲—, broadband.

broadband noise is higher than the blade passing frequency, BPF, and its harmonics. The large increase of total OAPWL in transonic is due to multiple pure tones, MPT, which are not completely removed from the broadband component. The departure from the theoretical law is 50 log 10 (M_{tip}) suggests there is another important parameter. On the right of Figure 15 a plot of reduced OAPWL versus the flow angle of attack on the rotor blades is shown (M_{hel} is the tip helical Mach number). Values collapse on a single straight line in subsonic, with a slope of 1·6 dB/deg. It can be inferred from this result that rotor self-noise dominates in upstream broadband radiation. The part at supersonic tip speeds has not the same shape, but this can be due to the remaining MPT. Indeed, other test series with an acoustic lining on the duct wall absorbs the MPT well, and broadband curves are continuous around $M_{tip} = 1$ which means that the generation mechanisms should be similar in subsonic and in supersonic. The next steps consist in comparing the results with RESOUND tests on low-noise research fans, and in developing a prediction method to compute fan broadband noise (by S. Lewy).

4. HELICOPTER NOISE

4.1. MAIN ACHIEVEMENTS IN THE FIELD OF HELICOPTER ROTOR NOISE RESEARCH

4.1.1. *Code development and validation*

The Kirchhoff code KIM [10] and the code FIM [11] based on the generalized Ffowcs Williams–Hawkings (porous surface) formulation respectively designed at ONERA in 1997 and 1998 have a high numerical efficiency thanks to the original integration technique [10]. They have been extended to deformable grids for proper adaptation to currently implemented CFD grids. Furthermore, the unsteady version of FIM, the last to be developed (for forward flight simulations) has been fully validated. In view of applications to acoustic flight tests and future design of low-noise flight procedures, the validation of the code CONGA [12] able to predict BVI noise using blade pressures measured by a small number of sensors has been completed on the basis of W.T. results [13]. It is intended to be applied to 2001 flight tests of the DLR BO105 helicopter for which unsteady main rotor blade pressures together with ground noise will be measured. In the framework of the

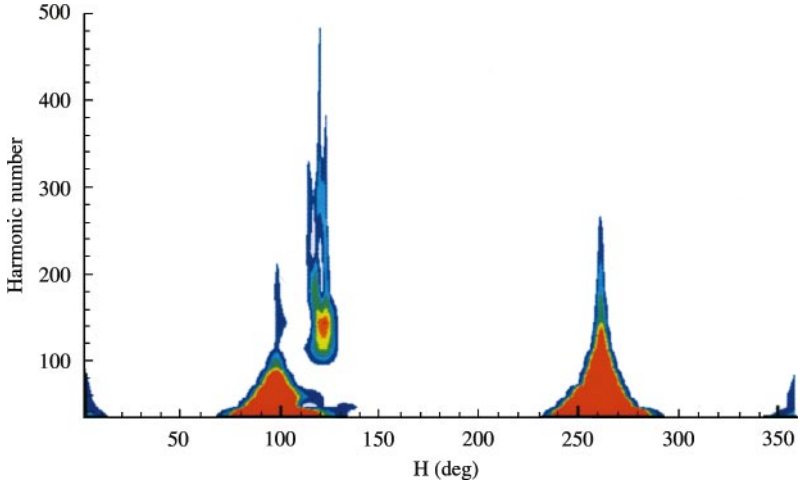

Figure 16. Characterization of BWI noise sources by wavelet analysis of HART test data (sample rotation) [16].

ER-ATO cooperation with DLR, a low-noise rotor geometry (with emphasis on low BVI noise and performance/dynamic constraints) was designed [14] and a highly instrumented model rotor manufactured and tested (together with a reference rotor) is the ONERA S1 Modane-Avrieux (S1MA) wind tunnel at high speed and in the DNW at moderate and low speed. Although the very satisfactory results reported in reference [15] verify the quiet rotor methodology applied, there is still room for improvement of the wake predictions particularly. The high-quality comprehensive data based acquired including extensive blade pressure, strain gauge, microphone and wake measurements (at DNW using LLS and PIV), is currently used for prediction/experiment correlations.

4.1.2. *Study of Blade Wake Interaction (BWI) noise of the main rotor*

A statistical analysis of HART BWI-related blade pressure fluctuations have been performed by means of the wavelet transform (see Figure 16). The study shows that BWI should be related to coherent structures expected to develop in the vicinity of the rotor vortices [16]. This conclusion is in opposition with current approaches which consider BWI as the result of a homogeneous and stationary random phenomenon. The next step of the study consists in numerical simulations of the development of such structures using a Navier–Stokes code, in co-operation with Le Havre University.

4.1.3. *Study of fenestron noise*

A comprehensive numerical and experimental program to study the noise generation mechanisms of Eurocopter helicopter fenestrons has been launched. The year 2000 has been devoted to the design of a pressure instrumented Dauphin fenestron in view of aeroacoustic flight tests (co-operation with Eurocopter and Istres Flight Test Center).

4.1.4. *Active rotor blade studies*

In co-operation with DLR and Eurocopter, numerical parametric studies of a scale-one rotor with active trailing edge flaps have been performed with respect to performance, noise and dynamics [17]. Studies of a model-scale rotor with such flaps have also been performed in view of future wind tunnel tests (by G. Rahier, J. Prieur and P. Spiegel).

4.2. DEVELOPMENTS OF THE K-ALGORITHM IN THE COMPUTATION OF EMISSION SURFACES

At CIRA the K-Algorithm, developed to integrate the Ffowcs Williams–Hawkings equation on a supersonic rotating domain [18] and to evaluate the high-speed impulsive (HSI) noise from helicopter rotors at high transonic regime [19], has been greatly revised and improved. At present the algorithm is able to determine the time evolution of a subsonic/supersonic emission surface, without any requirement about the geometrical symmetry of the rotating body and/or the microphone location, and in a very limited CPU time. This aim has been achieved by changing the structure of the code and through the development of a numerical procedure (named CIS: *Crossed Iteration Scheme*) devoted to the evaluation of the multiple emission times for supersonic sources [20]. The CIS is based

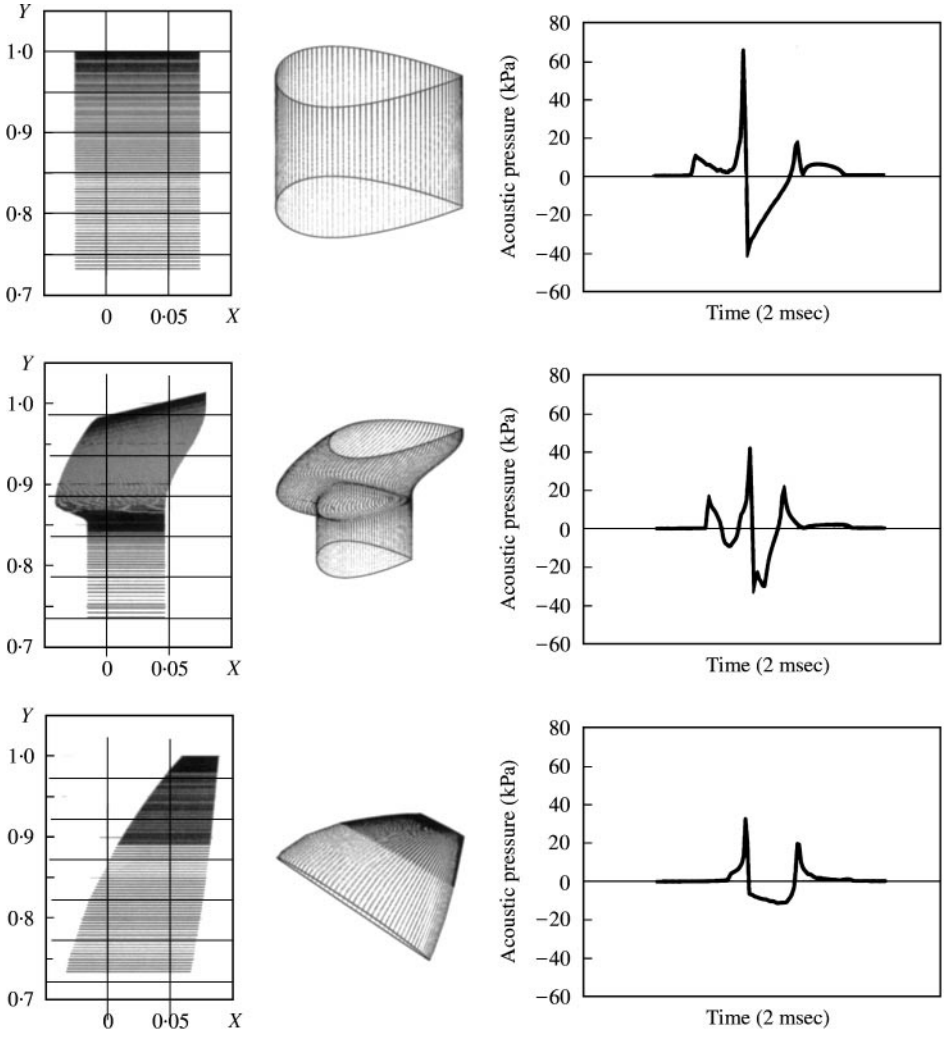

Figure 17. On the right: plan-view and 3-D-view of the numerical meshes used to test the K-Algorithm capability in computing a supersonic emission surfaces (Mach number between 0·95 and 1·3) and (left figures) the thickness noise signatures as determined at hovering condition and for an observer placed at 3 radii from rotor hub. Top, UH-1H untwisted blade; center, BERP-like blade; bottom, propeller blade.

on a double time loop sweeping forward and backward over the time period corresponding to the noise prediction of a source point and compared to the full iteration scheme required to find the roots of the *retarded function* (corresponding to the emission times) the CIS itself allows one to obtain a CPU time reduction greater than 95%. In order to test the capability of the K-Algorithm in computing the emission surface area and the different noise terms of the Ffowcs Williams–Hawkings equation, some critical tests have been examined. Figure 17 shows (on the left) both a planar and a 3-D-view of three blades, corresponding (from top to bottom) to a UH-1H untwisted blade with a uniform spanwise distribution of NACA0012 profile, and BERP-like blade with a complex tip shape and a high-speed propeller blade characterized by a significant variation of twist angle and chord along the span. The same Figure 17 shows (on the right) the thickness noise component as determined through the K-Algorithm, by accounting for a microphone placed in the rotor plane at a distance of 3 radii from the hub, and a range of the rotational Mach number between 0·95 and 1·3 (thus forcing the code to treat the critical region overlapping the sonic cylinder). Despite the occurrence of multiple emission times and the corresponding difficulties in modelling the emission surface, the signatures appear very smooth, thus proving the effectiveness of the procedure (by S. Ianniello).

5. TECHNIQUES AND METHODS IN AEROACOUSTICS

5.1. APPLICATION OF THE RAY-MODEL TO DUCT ACOUSTICS

In the framework of the European Brite-Euram DUCAT project, complementary methods have been developed for duct acoustics: BEM, FEM, coupled FEM/BEM, ray-acoustics, non-linear propagation model, extended reaction liner model. In practice, due to large CPU time consumption and memory requirements, the analysis of 3-D problems with numerical techniques is restricted to the low- and mid-frequency ranges. As a high-frequency approximation, the ray-model is an alternative method. Its capabilities to handle both in-duct propagation and radiation have been studied in the project [21]. Figure 18 illustrates a benchmark solution concerning the directivity pattern of a point source inside a duct. The comparisons with the LINDA modal approach [22] show that the ray model is valid when $kr = 7$ for rigid walls (Figure 18(a)), and when $kr = 35$ for lined walls (Figure 18(b)) (by P. Malbéqui).

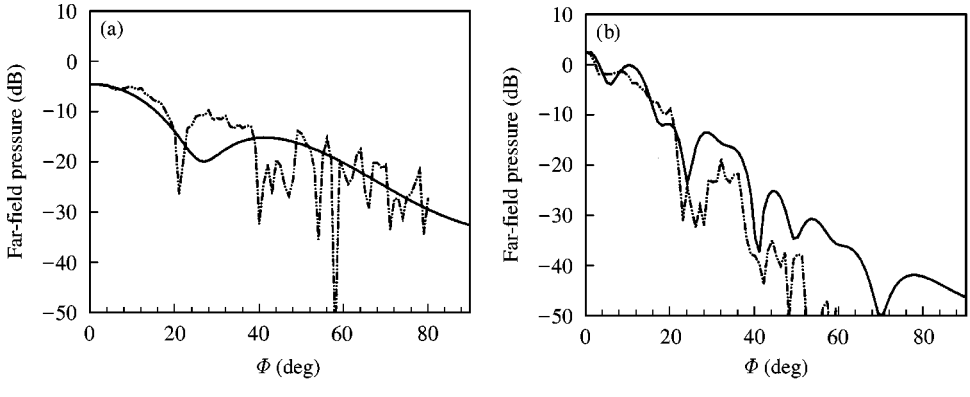

Figure 18. Directivity pattern of the sound radiation from a point source inside a duct. (a) $kr = 7$ rigid walls; (b) $kr = 35$, lined walls. ——, LINDA (NLR); –··–··–··–, Ray model (ONERA).

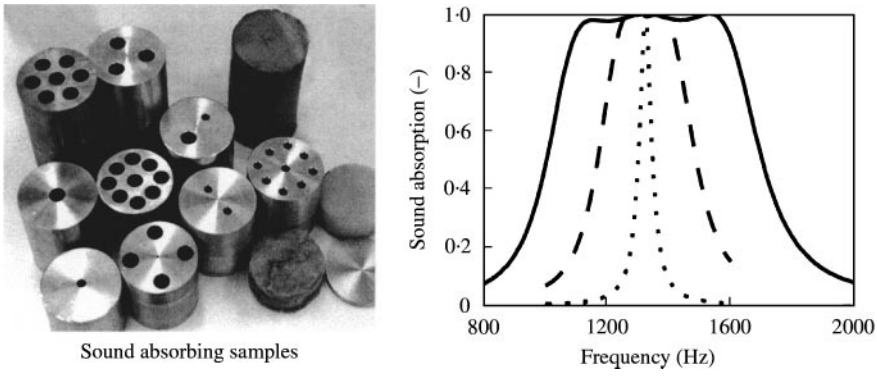

Figure 19. Sound absorbing samples with resonators and corresponding sound absorption coefficients (···, quarter-wavelength resonators; ——, two coupled tubes; –– three coupled tubes).

5.2. SOUND REDUCTION METHODS WITH PASSIVE AND/OR ACTIVE MEANS

Within the Applied Mechanics group of the Department of Mechanical Engineering at the University of Twente, research is carried out on coupling of structural vibrations and acoustics. The main objective is to investigate sound reduction methods with passive and/or active means. Overview is focused on the research on passive methods.

5.2.1. *Noise reduction with coupled prismatic tubes*

It is efficient to predict the effect of sound absorbing materials in advance for specific noise problems. For conventional sound absorbing materials, such as glass wool or foams, this is not an easy task. Therefore a well-defined model of a wall with a uniform distribution of resonators has been developed and validated experimentally. With the help of resonators, which consist of coupled tubes, a broadband absorption can be created for a predefined frequency range. Besides, in aggressive environments or at high temperatures special materials can be used [23, 24].

5.2.2. *Structural damping with double wall panels*

The vibrational behavior of light weight structures, such as a thin flexible panel, is strongly influenced by narrow air layers (see Figure 19). Structural vibrations and structure-borne sound can be reduced via this so-called squeeze film damping through viscous and thermal effects in the air layer. Analytical and FEM tools were developed. It is shown, both numerically and experimentally, that high damping coefficients for double wall panels can be obtained. The damping can be increased by placing barriers in the layer (see Figure 20). The vortices formed behind the barriers increase the dissipation of vibrational energy [25, 26] (by A. de Boer, H. Tijdeman, F. J. M. van der Eerden and T. G. H. Basten).

6. AIRCRAFT INTERIOR NOISE

6.1. THE REMOTE MICROPHONE TECHNIQUE FOR NACELLE ACTIVE NOISE CONTROL

During the RANNTAC project, the Laboratoire de Mécanique et d'Acoustique (L.M.A.) of CNRS worked on the concept of Remote Microphone Technique (RMT) for actively

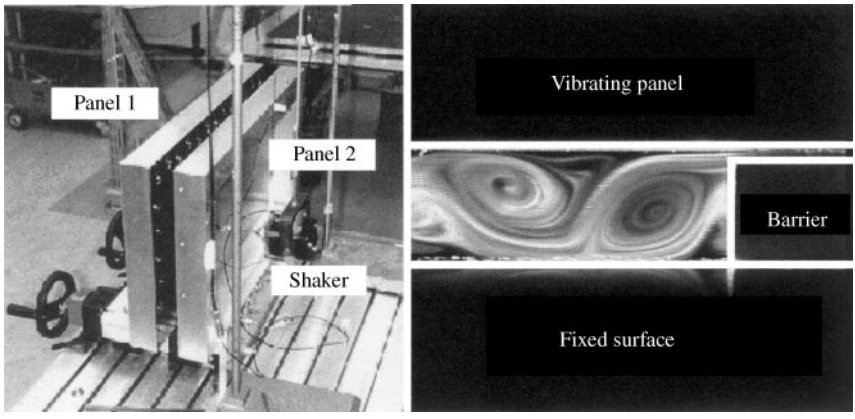

Figure 20. Experimental set-up for double wall panel measurements (left) and increased damping through vortices due to the presence of barriers (right).

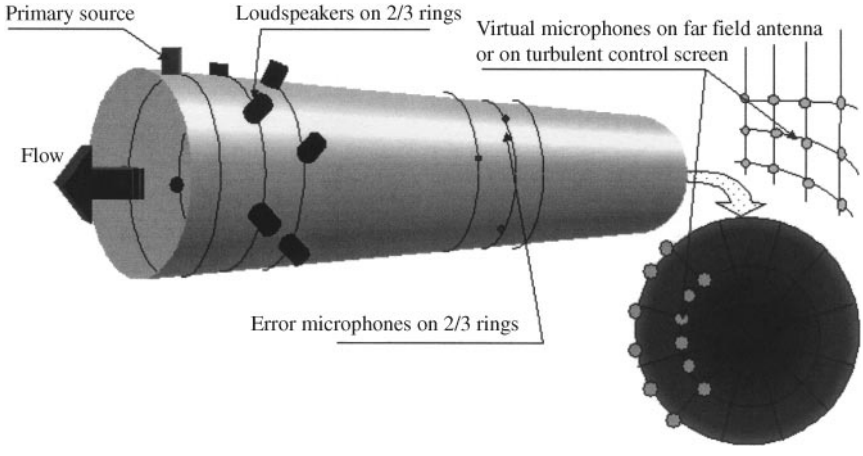

Figure 21. Transducer locations on the Snecma fan rig.

reducing the nacelle engine noise. The RMT algorithm is an Active Noise Control algorithm [27] allowing minimization of an acoustic field in some areas where error sensors cannot be located (far field of the engine noise, for example). It needs a preliminary identification phase where microphones are located in these "forbidden" areas and where transfer functions are measured between these "virtual" microphones and those of the control system (nacelle for example). During the control phase, an estimate of the instantaneous virtual field was done with the measured error sensor signals of the controller and with the identified transfer functions. A classical filtered x-LMS algorithm is then applied to this virtual acoustic field. During the ASANCA project [28], this algorithm had been implemented in aircraft to reduce turbofan noise in cabins and had given significant results during flying tests. In the RANNTAC project, the RMT algorithm has been tested on the SNECMA fan rig schematically shown in Figure 21. The virtual microphones were located on a farfield antenna at about 3 m of the inlet of the duct or on the turbulent control screen of this inlet. The secondary sources and the error microphones of the controller were put all around the duct surface. The controller used was a multichannel (16 outputs $\times$ 18 inputs)–multiprocessor (17 DSP) system, but the real-time computations needed by the RMT algorithm limited the control to only narrow bands of frequencies.

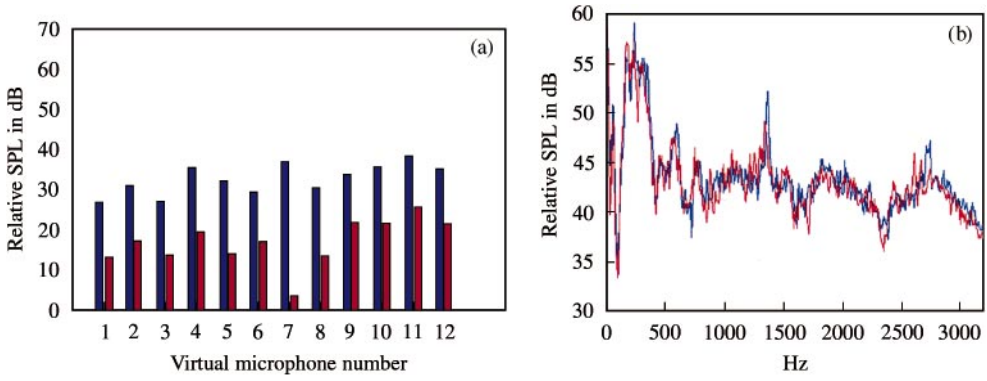

Figure 22. On the left: acoustic level measured on the virtual microphones for an RMT control of a 1320 Hz pure tone produced by a loudspeaker: ■, ANC off; ■, ANC on: —. On the right: mean spectrum of the acoustic field on the virtual microphones for an RMT control of the 1320 Hz pure tone produced by the nacelle engine. ▬, ANC off; ▬, ANC on.

The difficulties in this experiment came from the high frequencies to control (1500–3000 Hz), the high order of the modes propagating in the duct (> 7), and the large fluctuations of the engine speed during the control tests ($> 4\%$). The main conclusions of the tests were that the RMT algorithm is a valid concept for stationary fields as shown in the left Figure 22, in which the engine noise was replaced by a primary loudspeaker. With 12 secondary sources, 6 errors microphones and 12 virtual microphones located on the farfield antenna, 15–20 dB reduction of the directivity pattern of the primary field was obtained in a solid angle crossing the farfield antenna. With the engine noise and with the same transducers, the results are not so good (2–3 dB reduction only) due to the low tracking capability of the RMT algorithm when the primary noise fluctuates (right Figure 22). Recent investigations allow one to reduce drastically the calculation needed by the RMT algorithm. With these new improvements, broadband control should be possible that will probably authorize a greater robustness of the RMT algorithm to speed changes (by A. Roure, A. Albarrazin and M. Winninger).

REFERENCES

1. S. Oerlemans and P. Sijtsma 2000 *Sixth AIAA/CEAS Aeroacoustics Conference, Lahaina, HI*, 12–14 June. Effects of wind tunnel side-plates on airframe noise measurements with phased arrays.
2. J. W. Delfs 2001 *American Institute of Aeronautics and Astronautics Paper* 2001-2199. An overlapped grid technique for numerical simulation in Aeroacoustics.
3. H. A. Grogger, M. Lummer and T. G. Lauke 2001 *American Institute of Aeronautics and Astronautics Paper* 2001-2137. Simulation of leading edge noise of airfoils using CAA.
4. P. Költzsch and N. Kalitzin 1999 *Proceedings of Aeroacoustics Workshop SWING, Institut für Akustik und Sprachkommunikation, University of Technology Dresden, Germany*, October.
5. H. Körner and J. W. Delfs 2000 *Proceedings of Second Aeroacoustics Workshop SWING, Institut für Entwurfsaerodynamik, Deutsches Zentrum für Luft- und Raumfahrt, DLR Braunschweig, Germany*, October.
6. C. Bogey, C. Bailly and D. Juvé 2000 *American Institute of Aeronautics and Astronautics Paper* 2000-2009. Computation of the sound radiated by a 3-D jet using large eddy simulation.
7. C. Bogey, C. Bailly and D. Juvé 2000 *American Institute of Aeronautics and Astronautics Journal* **38**, 2210–2218. Numerical simulation of the sound generated by vortex pairing in a mixing layer. See also *American Institute of Aeronautics and Astronautics Paper* 99-1871.
8. X. Gloerfelt, C. Bailly and D. Juvé *C. R. Academy of Science*, t. 328, Série IIb 625–631. Calcul direct du rayonnemnt acoustique d'un écoulement affleurant une cavité.

9. S. LEWY 2000 *Seventh International Congress on Sound and Vibration*, *Garmisch-Partenkirchen*, *Germany*, July, pp. 1251–1258. Experimental study of fan brodband noise on a turbofan model.
10. G. RAHIER and J. PRIEUR 1997 53*rd Annual Forum of the American Helicopter Society*, *Virginia Beach*, *VA*, April–May. An efficient Kirchhoff integration method for rotor noise prediction starting indifferently from subsonically or supersonically rotating meshes.
11. J. PRIEUR and G. RAHIER 1998 *Fourth AIAA/CEAS Joint Aeroacoustics Conference*, *Toulouse*, *France*, June. Comparison of Ffowcs Williams–Hawkings and Kirchhoff rotor noise calculations.
12. P. SPIEGEL 1998 24*th European Rotorcraft Forum*, *Marseilles*, *France*, September. An iso-event spanwise interpolation technique for blade–vortex interaction noise prediction and analysis.
13. P. SPIEGEL 2000 56*th Annual Forum of the American Helicopter Society*, *Virginia*, *Beach*, *VA*, May. BVI noise prediction and analysis starting from blade pressures measured on a small number of points.
14. J. PRIEUR and W. SPLETTSTOESSER 1999 25*th European Rotorcraft Forum*, *Roma*, September. ERATO: an ONERA-DLR cooperative programme on aeroacoustic rotor optimisation.
15. W. SPLETTSTOESSER, B. VAN DER WALL, B. JUNKER, K. SCHULTZ, P. BEAUMIER, Y. DELRIEUX, P. LECONTE and P. CROZIER 1999 25*th European Rotorcraft Forum*, *Roma*, September. Wind tunnel test results and proof of design for an aeroacoustically optimised rotor.
16. E. BOUCHET and G. RAHIER 2000 56*th Annual Forum of the American Helicopter Society*, *Virginia Beach*, *VA*, May. Structure of the blade pressure fluctuations generated by helicopter rotor blade–wake interaction.
17. P. LECONTE and R. KÜBE 2000 *Second ONERA-DLR Aerospace Science Meeting*, *Berlin*, June. Main rotor active flaps: numerical assessment of noise and vibration reduction.
18. S. IANNIELLO 1999 *American Institute of Aeronautics and Astronautics Journal* **37**, 1040–1047. An algorithm to integrate the FW-H equation on a supersonic rotating domain.
19. S. IANNIELLO 1999 *American Institute of Aeronautics and Astronautics Journal* **37**, 1048–1054. Quadrupole noise predictions through the Ffowcs Williams–Hawkings equation.
20. S. IANNIELLO 2000 *Sixth AIAA/CEAS Aeroacoustics Conference*, *Lahaina*, *HI*, 12–14 June. Developments of the K-algorithm in the computation of the HSI noise from rotors and propellers.
21. P. MALBIÉQUI 1998 *DUCAT S.T*1.5, *ONERA Technical Report*, *RT* 26/3641 *DSNA/Y*, October. Application of the ray-model to duct acoustics.
22. S. W. RIENSTRA 1984. *Journal of Sound and Vibration* **94**, 267–288. Acoustic radiation from a semi-infinite annular duct in a uniform subsonic mean flow.
23. F. J. M. VAN DER EERDEN 2000 *Ph.D. Thesis*, *University of Twente*. Noise reduction with coupled prismatic tubes.
24. H. E. DE BREE, F. J. M. VAN DER EERDEN and J. W. VAN HONSCHOTEN 2000 *ISMA* 25 *Conference on Noise and Vibration Engineering*, *Leuven*, *Belgium.* A novel technique for measuring the reflection coefficient of sound absorbing materials.
25. T. G. H. BASTEN and H. TIJDEMAN 2000 *ISMA* 25 *Conference on Noise and Vibration Engineering*, *Leuven*, *Belgium.* Damping of structural vibrations by vortex shedding.
26. T. G. H. BASTEN, P. J. M. VAN DER HOOGT, R. M. E. J. SPIERING and H. TIJDEMAN 2001 *Journal of Sound and Vibration* (accepted). On the acousto-elastic behaviour of double wall panels with a viscothermal air layer.
27. A. ROURE, A. ALBARRAZIN and M. WINNINGER 1999 *ACTIVE* 99, 1233–1244. The remote microphone technique for active noise control.
28. D. JUVÉ 1999 *Journal of Sound and Vibration* **227**, 321–342. Aeroacoustic research in Europe: the CEAS-ASC report on 1998 highlights.